

# HALO OCCUPATION DISTRIBUTIONS OF MODERATE X-RAY AGNS FORMED THROUGH MAJOR AND MINOR MERGERS IN A $\Lambda$ -CDM COSMOLOGY

L. Altamirano-Dévora, T. Miyaji, H. Aceves, A. Castro, R. Cañas, and F. Tamayo

Instituto de Astronomía, Universidad Nacional Autónoma de México, Ensenada, Baja California, México

Received June 8 2015; accepted October 14 2015

## RESUMEN

Motivados por la forma de la distribución de ocupación de halos (HOD) de núcleos activos de galaxias (AGNs) seleccionados por rayos X en el campo de COSMOS, inferida por Allevato et al., investigamos la HOD de núcleos activos de galaxias en rayos X moderados (mXAGNs) usando un modelo basado en la fusión entre halos de materia oscura (DMHs) en una cosmología  $\Lambda$ CDM. La HOD y las densidades numéricas de los mXAGNs simulados en  $z = 0.5$  en los escenarios anteriores se calcularon y compararon con los resultados de Allevato et al. Encontramos un comportamiento similar entre las HODs simuladas de fusiones mayores y menores, y la observada para los mXAGNs. El resultado principal es que las fusiones menores, en contra de lo que se podría esperar, pueden desempeñar un papel importante en la activación de los mAGNs.

## ABSTRACT

Motivated by the shape of the halo occupation distribution (HOD) of X-ray selected AGNs in the COSMOS field recently inferred by Allevato et al., we investigated the HOD properties of moderate X-ray luminosity active galactic nuclei (mXAGNs) using a simple model based on the merging activity between dark matter halos (DMHs) in a  $\Lambda$ CDM cosmology. The HODs and number densities of the simulated mXAGNs at  $z = 0.5$ , under the above scenarios were compared with the results of Allevato et al. We found that the simulated HODs of major and minor mergers, and the observed HODs of mXAGNs are consistent. Our main result is that minor mergers, contrary to what one might expect, can play an important role in the activity of mAGNs.

*Key Words:* galaxies: active — galaxies: halos — methods: numerical

## 1. INTRODUCTION

Studies of AGN host galaxies are fundamental to understand the physical mechanisms that trigger AGN activity and that govern the fuelling rate of the central black hole (e.g., Gilmour et al. 2009; Alexander & Hickox 2012; Beckmann & Shrader 2012).

The observed correlation between the mass of the central BH and the velocity dispersion ( $\sigma$ ) of the bulge of the host galaxy suggest a strong connection between galaxy evolution and BH activity (e.g., Gebhardt et al. 2000; Merritt & Ferrarese 2001; Tremaine et al. 2002; Kormendy & Ho 2013). This activity is related to the accretion of material onto the central engine triggered by, for example: the merger of gas-rich galaxies (e.g., Silk & Rees

1998; Springel et al. 2005b; Hopkins et al. 2008), bar-driven inflows (e.g., Jogee 2006), disk instabilities (Bournaud et al. 2011), collisions with molecular clouds (Hopkins & Hernquist 2006), stellar winds from evolved stars (Ciotti & Ostriker 2007), and the transportation of gas to galactic centers by supernova explosions (Chen et al. 2009) or a combination of these effects.

Mergers and strong interactions can induce substantial gravitational torques on the gas content of a galaxy, depriving it of its angular momentum, and leading to gas inflows and the buildup of huge reservoirs of gas at its center (e.g., Hernquist 1989; Barnes & Hernquist 1991, 1996; Mihos & Hernquist 1996; Springel et al. 2005b; Cox et al. 2006, 2008; Di

Matteo et al. 2007). Major galaxy mergers are very efficient in moving gas to galaxy centers due to the generation of large torques. Visual inspections of host galaxies of AGNs (Treister et al. 2012) have found that the more luminous AGNs show recent merger features, while such features are not commonly seen in the less luminous AGNs, which appear to be driven by another process. Low luminosity AGNs could also be triggered in non-merger scenarios (e.g., Milosavljević et al. 2006; Hopkins & Hernquist 2006, 2009), and probably also by the interaction with very small satellites (total mass ratio of about 1:100), as recently suggested by Ramón-Fox & Aceves (2014).

The main process triggering AGN activity could be a function of redshift and/or halo mass. The anti-hierarchical evolution of AGNs (or AGN downsizing), in which the number density of low luminosity AGNs comes later in the universe than high-luminosity ones (Ueda et al. 2003; Hasinger et al. 2005; Ueda et al. 2014), is probably not consistent with the theoretical predictions of a major merger AGN triggering scenario such as the one suggested by Wyithe & Loeb (2003). Some recent theoretical studies based on cosmological simulations suggest the necessity of a combination of merger and secular processes (e.g. Draper & Ballantyne 2012), or of hot-halo accretion and star-burst induced triggering (Fanidakis et al., 2012) to explain the evolution of the luminosity function of AGNs and their clustering properties (Fanidakis et al. 2013). These results suggest that one or more mechanisms other than major mergers are at least partially responsible for triggering AGN activity.

Bias measurements of large scale AGN show that mXAGNs are on average associated with more massive DMHs than more luminous QSOs (e.g., Miyaji et al. 2007; Krumpke et al. 2010; Allevato et al. 2011). While the typical masses of DMHs associated with QSOs [ $M_{\text{DMH}} \approx 10^{12-13} h^{-1} M_{\odot}$ ; Porciani et al. (2004); Croom et al. (2005); Hopkins et al. (2007); Coil et al. (2007); da Ângela et al. (2008); Mountrichas et al. (2009)] are consistent with a major merger triggering scenario (e.g., Shen 2009), those associated with mXAGNs are typically more massive, with  $M_{\text{DMH}} \approx 10^{13-14} h^{-1} M_{\odot}$  (i.e., the mass scale of rich groups and poor clusters), and results from Allevato et al. (2011) suggest that secular processes could trigger mXAGNs.

Cosmological simulations are an important tool to understand the distribution of dark matter in the universe, and the co-evolution and growth of BHs

with respect to their host galaxies (e.g., Sijacki et al., 2007; Di Matteo et al., 2008; Thacker et al., 2006). In  $N$ -body simulations, the requirement of associating the dark matter with galaxy distributions has to be satisfied (e.g., Pujol & Gaztañaga, 2014). Studies of AGN clustering using cosmological simulations have been carried out using the halo model (e.g., Thacker et al., 2009; Degraf et al., 2011) or the BH continuity equation approach (e.g., Lidz et al., 2006; Bonoli et al., 2009; Shankar et al., 2010). The HOD method allows to distinguish between AGN evolution models (e.g., Chatterjee et al., 2012). It has been used by several authors to interpret AGN and quasar clustering measurements from direct counts of AGNs within groups of galaxies (e.g., Wake et al., 2008; Shen et al., 2010; Miyaji et al., 2011; Starikova et al., 2011; Krumpke et al., 2012; Allevato et al., 2012; Richardson et al., 2012; Kayo & Oguri, 2012; Chatterjee et al., 2013; Krumpke et al., 2014).

The environment of AGN and, in particular, the mass of the typical DMHs in which they reside, is a powerful diagnostic of the physics that drive the formation of super massive black holes (SMBHs) and their host galaxies (e.g., Mountrichas & Georgakakis, 2012). By modeling the mean AGN occupation at  $z = 0.5$ , Allevato et al. (2012) found that the host halos of these AGNs have a DMH with a mass  $M_{\text{DMH}} \geq 10^{12.75} h^{-1} M_{\odot}$ , that is, a DMH mass corresponding to galaxy groups (Eke et al., 2004). This result agrees with studies by Georgakakis et al. (2008) and Arnold et al. (2009), which present evidence that AGNs at  $z \approx 1$  are frequently found in groups. Moreover, Miyaji et al. (2011) estimated a shape of the HOD of X-ray selected AGN that suggests that the AGN satellite fraction increases slowly with  $M_{\text{DMH}}$ , in contrast with the satellite HOD of low luminosity limited samples of galaxies. For these galaxies, Allevato et al. (2012) found that the slope  $\alpha$  of the HOD distribution of satellite AGNs had a value of  $\alpha_s \leq 0.6$ , suggesting a picture in which the average number of satellite AGNs per halo mass decreases with the halo mass.

Considering that  $\alpha \approx 1$  is the value inferred for galaxies in general (e.g., Coil et al. 2009; Zehavi et al. 2011), the study of the HOD of AGNs suggests that the AGN fraction in galaxies decreases with increasing DMH mass. The reason for this may be that the cross-section of the merger between two galaxies decreases with increasing relative velocity and, thus, that the merging frequency is suppressed in a group/cluster environment with high velocity dispersion (Makino & Hut 1997). In addition, gas processes such as ram-pressure stripping of cold gas

in galaxies by hot intragroup/intracluster gas suppresses star formation activities that may feed AGN (Gunn & Gott 1972).

In this work we investigated a scenario where satellite subhalos, from  $N$ -body cosmological simulations harbor mXAGNs within a group/cluster-sized parent halo of  $M_{\text{DMH}} \geq 10^{12.75} h^{-1} M_{\odot}$ , and were triggered by either a major or minor merger. We estimated the HODs of the simulated mXAGNs and compared them with the inferred HOD obtained by Allevato et al. (2012) and Miyaji et al. (2015) in order to see if we could reproduce such results by using this approach. In brief, we used a simple approach for coupling cosmological simulations of  $\Lambda$ CDM with semi-analytical results to determine the HOD of our numerical AGNs.

The outline of the paper is as follows. In § 2 we describe the method used in this work to determine AGN candidates in cosmological simulations to estimate their HOD. In § 3 we show our results; we discuss them in § 4, and, finally, in § 5 we indicate our main conclusions. Throughout this paper we assume a matter density  $\Omega_{\text{m}} = 0.266$ , dark energy density  $\Omega_{\Lambda} = 0.734$ ,  $H_0 = 72 \text{ km s}^{-1} \text{ Mpc}^{-1}$  and mass RMS fluctuation  $\sigma_8 = 0.816$  consistent with the WMAP7 results of Larson et al. (2011).

## 2. MODEL

In this section, we describe the cosmological simulations and the semi-analytical procedure used to establish an association between satellite subhalos and the observational properties of mXAGNs; we then describe the criteria used to determine when a merger occurs, as well as the actual computation of the HOD.

### 2.1. Numerical simulations

We performed a set of five similar  $N$ -body cosmological simulations within the  $\Lambda$ CDM model, each differing from the others in the random seed used to generate the initial conditions.

Each simulation box had a co-moving length of  $L = 100 h^{-1} \text{ Mpc}$  with  $N_{\text{p}} = 512^3$  dark matter particles, each with a mass of  $m_{\text{p}} = 6 \times 10^8 h^{-1} M_{\odot}$ . The initial conditions were generated using 2nd-order Lagrangian Perturbation Theory (e.g., Crocce et al. 2006), starting at a redshift of  $z = 50$ . The initial linear power spectrum density was obtained from the cosmic microwave background code CAMB (Lewis et al. 2000).

The  $N$ -body simulations were carried out using the publicly available parallel Tree-PM code GADGET2 (Springel 2005). The simulations were run with a softening length of  $\varepsilon = 20 h^{-1} \text{ kpc}$ . Two cosmological simulations were re-run with  $\varepsilon = 1 h^{-1} \text{ kpc}$ ; no change was noted in the HOD results. The change in  $\varepsilon$  can affect the properties of the inner profiles of the halos, but that study is out of the scope of the present paper.

### 2.2. Halo finder algorithm

We identified DMHs and subhalos using the Amiga Halo Finder (AHF) code, which locates halo centers using an adaptive mesh refinement (AMR) approach. In brief, this code finds prospective halo centers, collects particles possibly bound to the center, removes unbound particles and calculates halo properties (Knollmann & Knebe 2009; Knebe et al. 2011)<sup>1</sup>. Virial masses are defined at an overdensity of  $200\rho_{\text{c}}$ , where  $\rho_{\text{c}}$  is the critical density of the universe. We used a minimum number of particles  $N_{\text{p}} = 100$  to define a bound halo.

As mentioned in § 1, we are interested in DMH with a virial mass of  $M_{\text{DMH}} \geq 10^{12.75} h^{-1} M_{\odot} \equiv M_{\text{th}}$  at a  $z = 0.5$  snapshot, in which mXAGNs preferentially reside (Allevato et al. 2012; Padmanabhan et al. 2009). This is consistent with the HOD modeling of the cross-correlation function between ROSAT all-sky Survey AGNs and low-luminosity red galaxies (Miyaji et al. 2011). We focused our attention on those DMH that reside at a non-central location of the host halo.

Halos with  $M_{\text{DMH}} > M_{\text{th}}$  at redshift  $z = 0.5$  are called host-halos (HHs hereafter). We identified subhalos belonging to these HHs, and selected the subhalos that are satellites (subhalo-host, SH); see Figure 1.

### 2.3. Connection of subhalos to mXAGN

Several approximate methods to assign AGN or quasar activity to halos are described in the literature. For example, Croton (2009) uses the  $M_{\text{BH}}\text{-}\sigma$  relation by requiring the reproduction of the observed luminosity function of quasars, using the abundance matching technique to “turn-on” halos in the *Milennium* simulation (Springel et al. 2005a). Conroy & White (2013) invoked an empirical model of the halo population and  $M_{\text{BH}}\text{-}M_{\text{gal}}$  in which quasars are treated as light bulbs to match the luminosity function of quasars.

<sup>1</sup><http://popia.ft.uam.es/AHF/Download.html>

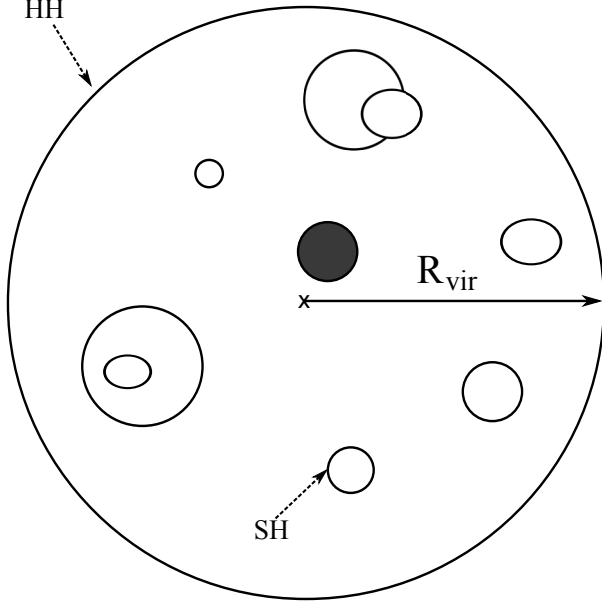


Fig. 1. This schematic diagram illustrates the host–halo (HH of mass  $M_{\text{th}}$ ) as a circle with virial radius;  $R_v$ . Several subhalos (SHs) are depicted inside  $R_v$ . The central subhalo is identified as the closest to the center of the host-halo (dark filled circle) while the others are considered satellite subhalos (empty circles).

In this section we explain the different scaling relations used in our analysis to establish an association between the subhalos and the observational properties of AGNs.

### 2.3.1. Black hole mass

The central velocity dispersion  $\sigma$  of each SH is associated with the black hole mass  $M_{\text{BH}}$  (Kormendy & Ho 2013) by:

$$\log\left(\frac{M_{\text{BH}}}{M_0}\right) = -0.50 + 4.38 \log\left(\frac{\sigma}{\sigma_0}\right), \quad (1)$$

where  $M_0 = 10^9 h^{-1} M_\odot$  and  $\sigma_0 = 200 \text{ km s}^{-1}$ .

### 2.3.2. Assigning the Eddington ratio

Given a  $M_{\text{BH}}$ , an Eddington ratio ( $\lambda_{\text{Edd}}$ ) can be defined as:

$$\lambda_{\text{Edd}} = \frac{L_{\text{bol}}}{L_{\text{Edd}}(M_{\text{BH}})}, \quad (2)$$

where  $L_{\text{bol}}$  is the bolometric luminosity and  $L_{\text{Edd}}(M_{\text{BH}})$  is the Eddington luminosity, which is proportional to  $M_{\text{BH}}$ .

Combining equation 2 with the data provided in Table 2 from Lusso et al. (2012), we can obtain the X-ray luminosity as:

$$\log[L_{\text{bol}}/L_{\text{band}}] = a_1 x + a_2 x^2 + a_3 x^3 + b, \quad (3)$$

where  $L_{\text{band}}$  corresponds to the 0.5-2 keV band luminosity,  $x = \log L_{\text{bol}} - 12$ ;  $a_1$ ,  $a_2$ ,  $a_3$  and  $b$  are bolometric correction coefficients.

We need to mimic a population of AGNs representing mXAGNs within our simulations and construct the HOD to compare it with the observed mXAGNs HOD by Allevato et al. (2012). To do this, we used a representative value of  $\lambda_{\text{Edd}} = 0.1$ ,  $a_1 = 0.248$ ,  $a_2 = 0.061$ ,  $a_3 = -0.041$  and  $b = 1.431$ , restricting the calculations only to subhalos with  $L_x \geq 10^{42.4} h^{-2} \text{ erg s}^{-1}$ .

Using equations (1-3), we obtained the black hole mass threshold  $M_\bullet$ , which we used to obtain the number density of subhalos with active or dormant black holes,  $n_{(\geq M_\bullet)}$ . We also considered a  $z = 0.5$  snapshot, which is the median redshift of the sample used by Allevato et al. (2012). We designated the black holes as active or dormant depending on whether they had undergone a galaxy merger within the AGN lifetime  $\tau_{\text{AGN}}$  in the past.

## 2.4. Determining the AGN lifetime

Instead of using the abundance matching technique, we selected the duty cycle (e.g., Cappelluti et al. 2012) as an indicator that the subhalo was turned on. In the following, we took a simple approach and assumed that all AGNs observed at  $z = 0.5$  above the luminosity threshold, are shining at  $\lambda_{\text{Edd}} = 0.1$  during their lifetime,  $\tau_{\text{AGN}}$ .

Using the X-ray [2–10 keV] band luminosity function (XLF) of AGNs by Miyaji et al. (2015), and the model of the distribution function of absorbing column density by Ueda et al. (2014), in combination with the results of Allevato et al. (2012), we estimated the number density of AGNs, including absorbed (within the Compton-thin range, i.e.,  $N_{\text{H}} < 10^{24} [\text{cm}^{-2}]$ ) and unabsorbed ones, above the intrinsic (i.e., before absorption) [0.5–2 keV] B-band luminosity of  $L_x \geq 10^{42.4} h^{-2} \text{ erg s}^{-1}$ . We obtained:

$$n_{\text{AGN}} \sim 4.2 \times 10^{-5} h^3 \text{ Mpc}^{-3}. \quad (4)$$

The idea behind using the 2-10 keV luminosity function is that the 0.5-2 keV sample used by Allevato et al. (2012) is highly biased against absorbed

AGNs. In order to estimate more accurately the lifetime of AGNs, we require the number density of both absorbed and unabsorbed AGNs. For simplicity, we here assume that the satellite HODs of absorbed and unabsorbed mXAGNs have the same shape.

To constrain the number density of AGNs that can be observed at  $z = 0.5$ , we used the timescale  $\tau_{\text{AGN}}$ , which indicates when the mXAGNs were activated. We estimated the AGN lifetime  $\tau_{\text{AGN}}$  as follows:

$$\tau_{\text{AGN}} \approx \frac{n_{\text{AGN}}}{n_{(\geq M_{\bullet})}} \times \tau_{\text{age}(z=0.5)}, \quad (5)$$

where  $n_{\text{AGN}}$  is the observed number density of X ray AGNs,  $n_{(\geq M_{\bullet})}$  is the simulated number of SHs with BH mass threshold (active or dormant), and  $\tau_{\text{age}(z=0.5)}$  is the age of the universe at  $z = 0.5$ .

### 2.5. Criteria for identifying major and minor mergers

We identified major and minor mergers at the redshift corresponding to the AGN lifetime  $\tau_{\text{AGN}}$  before  $z = 0.5$ , so that the AGNs triggered by the mergers during this interval were still active at  $z = 0.5$  under these scenarios.

We defined a mass ratio  $\mu = M_2/M_1$  of the progenitors, where  $M_2 > M_1$ . We considered mergers with mass ratios  $0.25 \leq \mu \leq 1.0$  as major and those with  $0.1 \leq \mu < 0.25$  as minor mergers. In order to identify a merger event between two progenitors, the following criteria have to be met (e.g., Farouki & Shapiro 1981):

1. Their relative velocity  $V_{12} = |V_1 - V_2|$  is less than the average (rms) velocity dispersion of both halos  $\langle V_{\text{rms}} \rangle$ ; i.e.,  $V_{12} \leq \langle V_{\text{rms}} \rangle$ .
2. Their relative physical separation  $R_{12} = |r_1 - r_2|$  is less than the sum of the virial radius of both halos:  $R_{12} \leq R_{v1} + R_{v2}$ .

To find these merger candidates, we used the *MergerTree* tool included in the AHF software; we tagged as progenitor the halo that contained the greatest fraction of SH particles (Libeskind et al. 2010). After this initial identification of the merger event, we verified that a merger event occurred by inspecting the snapshots.

### 2.6. Simulated HOD

The following formula was used in order to estimate the HOD of mXAGNs:

$$N(M_{\text{th}}) = \frac{n_{\text{HHagn}}}{n_{\text{HH}}}, \quad (6)$$

where  $n_{\text{HHagn}}$  is the number density of HHs that have a SH that has undergone a major or minor merger and that has a  $M_{\text{BH}} \geq M_{\bullet}$ , and  $n_{\text{HH}}$  is the total number density of HH (defined in § 2.2) in simulations. The mass bin size used was  $\Delta \log M_{\text{th}} 0.4$ .

## 3. RESULTS

Before presenting our results, we should note the following: the HOD measured by Allevato et al. (2012) was evaluated at  $z = 0$ ; their measurement was made over a sample extending up to  $z \approx 1$  that was corrected for the 0.5-2 keV XLF and its luminosity-dependent evolution, as indicated by Ebrero et al. (2009). Their sample is more representative of  $z \approx 0.5$  than of  $z \approx 0$ .

To make a comparison with our results, we back-corrected their HOD to  $z \approx 0.5$  in the following way: the luminosity-dependent density evolution (LDDE) model, describing the 0.5-2 keV XLF derived by Ebrero et al. (2009), indicates that the number density grows as  $\propto (1+z)^{3.38}$  up to  $z \approx 0.8$  at all luminosities. Thus, we converted the HOD at  $z = 0$  to  $z = 0.5$ . The HOD results from multiplying by  $(1+0.5)^{3.38} = 3.9$  at all DMH masses. Furthermore, since the Allevato et al. (2012) sample in the 0.5-2 keV band is highly biased against obscured AGNs, we further multiplied the HOD by a factor of 2 to account for the obscured AGN contribution using the recent 2-10 keV XLF model by Miyaji et al. (2015). Figure 2 shows our results for the HOD of major and minor mergers and the corrected form of the HOD at a redshift of  $z = 0.5$ .

The slope of the HOD shows the same trend for both minor and major mergers at masses  $\lesssim 5 \times 10^{13} h^{-1} M_{\odot}$ . However, at larger masses, the minor and major HODs show a somewhat different behavior, with the major merger HOD increasing and the minor one tending to be flat (Figure 2). To make a comparison with the slope ( $\alpha_s$ ) found by Allevato et al. (2012), we used the same occupation function model, which is described by:

$$\langle N_{\text{sat}} \rangle (M_{\text{h}}) = f'_a \left( \frac{M_{\text{h}}}{M_1} \right)^{\alpha_s} \exp(-M_{\text{cut}}/M_{\text{h}}); \quad (7)$$

where  $f'_a$  is a normalization,  $M_1$  is the halo mass at which the number of central AGN is equal to that of satellite AGNs ( $\log M_1 = 13.8 M_{\odot}$ ), and  $M_{\text{cut}}$  is a cut-off mass scale ( $\log M_{\text{cut}} = 13.4 M_{\odot}$ ).

The fitted slope for the minor merger case was  $\alpha_s = 0.10 \pm 0.09$  and  $\alpha_s = 0.20 \pm 0.18$  for the major merger; both can be compared with the slope

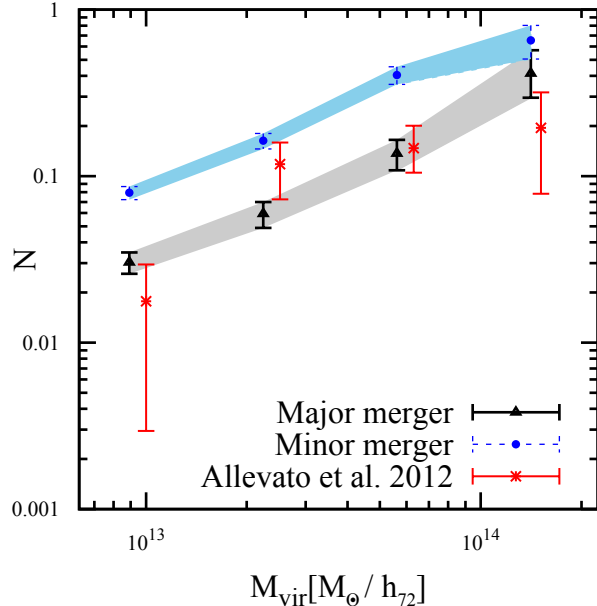


Fig. 2. The HOD of the number of hosts that harbor a mXAGN triggered by either a major (blue dots) or minor merger (black triangles), and the inferred HOD of satellites mXAGNs by Allevato et al. (2012) (red asterisks). The latter was corrected by an evolution factor and by addition of the unabsorbed AGN estimation by Miyaji et al. (2015). Error bands were calculated as indicated in the text. The color figure can be viewed online.

observed by Allevato et al. (2012)  $\alpha_s \leq 0.6$  (Table 1). The slope of the minor merger HOD is closer to that of the mXAGN HOD than to that of the major merger case. However, both slopes are consistent with the observations.

The errors in Figure 2 were derived as follows: if  $n_{\text{HHagn}}$  was less than 15, we estimated  $1\sigma$  errors using the equations (7) & (12) of Gehrels (1986). If  $n_{\text{HHagn}} \geq 15$ , we estimated the  $1\sigma$  errors by  $\sqrt{n_{\text{HHagn}}}$ .

#### 4. DISCUSSION

Different numerical studies have addressed the triggering of AGNs, in particular by mergers between galaxies, since it is a naturally expected contributing process (e.g., Sanders et al. 1988; Hopkins et al. 2006). Major mergers are considered to activate QSO's, a situation that has been studied through hydrodynamical cosmological simulations, measurements of their clustering properties and of the properties of AGNs (Sijacki et al. 2007; Di Matteo et al. 2008; Marulli et al. 2009; Ciotti et al. 2010; Degraf et al. 2011; Chatterjee et al. 2012; Van Wassenhove et al. 2012; Krumpe et al. 2015).

TABLE 1

NUMBER DENSITIES AND HOD SLOPES

Mechanism	$n_{\text{agn}}$	$\alpha_s$
Major	$2.28 \times 10^{-5}$	$0.20 \pm 0.18$
Minor	$5.96 \times 10^{-5}$	$0.10 \pm 0.09$
Observed <sup>1</sup>	$4.2 \times 10^{-5}$	$0.22^{+0.41}_{-0.29}$

<sup>1</sup>Allevato et al. (2012).

However, Schawinski et al. (2011) found that most of the quasars in their sample have disk-like morphologies, suggesting that a secular evolution mechanism could drive the activity to this type of AGNs. Moreover, if only major mergers turn out to be important at high-redshifts, the AGNs should probably reside in more elliptical-shaped galaxies (Cisternas et al. 2011). In contrast, Lee et al. (2012) and Cisternas et al. (2013) found that the bar-driven gas and the gas that could trigger nuclear activity do not correlate; a mechanism discussed in particular by Wyse (2004).

Stochastic accretion models have been thought to trigger the mechanism of low/moderate AGNs (Hopkins & Hernquist 2006; Hopkins et al. 2014; Kocevski et al. 2012). Thus, secular evolution (e.g., Ehlert et al. 2015) has become an important scenario, as well as minor mergers (De Robertis et al. 1998; Hernquist & Mihos 1995; Taniguchi 1999; Kendall et al. 2003; Hopkins & Hernquist 2009; Karouzos et al. 2014), owing to the fact that injection of gas is recurrent and keeps the accretion going, which can explain the non-disk AGNs and can in some cases influence the growth of SMBH (e.g., Kaviraj 2014). As intermediate mergers are more common than major mergers (e.g., Tapia et al. 2014), they may also play a role. Recognizing that the main triggering mechanism is not obvious in all types of AGNs, we conducted a study in which mXAGNs are triggered by either major or minor mergers using the HOD formalism and a simplified model.

It is difficult to estimate the precise time of the merger, and, therefore, the time when the BH will be activated. Using the dynamical friction time (e.g., Hopkins et al. 2010) to estimate when the progenitors merge, causes an important overestimation compared to following as closely as possible the evolution in time of the subhalos in our cosmological simulations. Furthermore, results by Jiang et al. (2014) show that it is not adequate to use a single time scale to infer when the merging takes place.

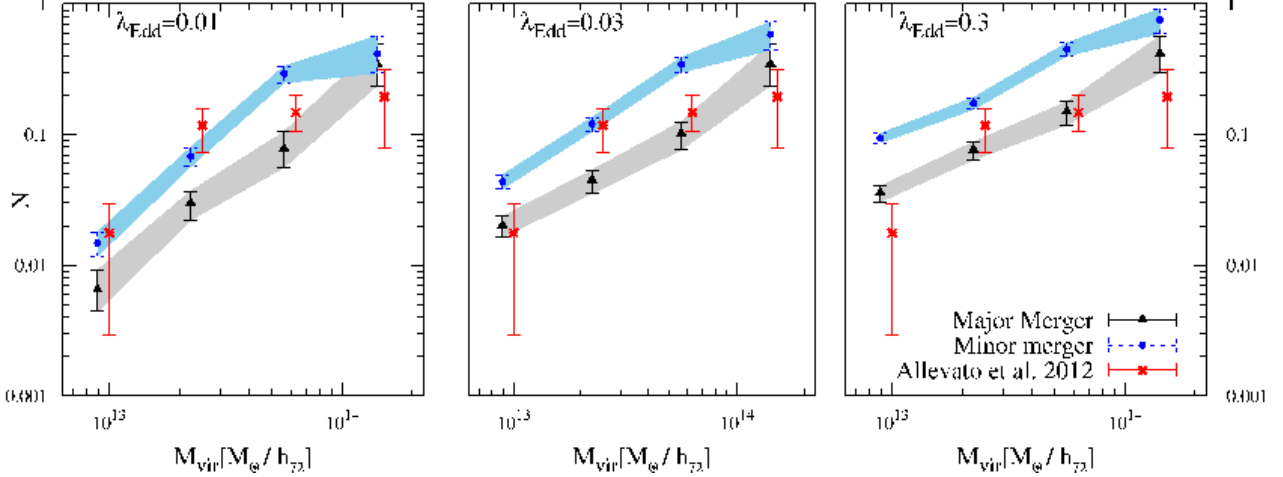


Fig. 3. The HOD of different values of  $\lambda_{Edd}$ , the number of hosts that harbor a mXAGN triggered by either a major (blue dots) or minor merger (black triangles), and the inferred HOD of satellite mXAGNs according to Allevato et al. (2012) (red asterisks). The color figure can be viewed online.

In spite of the wide range of probable environments in which AGNs reside (Villarreal & Korn 2014; Karouzos et al. 2014; Leauthaud et al. 2015), in this work we assumed that the host/environment of the mXAGN has a group-like halo mass, as indicated by some observations (e.g., Allevato et al. 2012; Silverman et al. 2014). We concentrated our attention on the mXAGNs that reside in non-central subhalos. The connection between galaxies and DMHs has been established in different ways: assigning the stellar mass of the galaxies to DMHs (Degraf et al. 2011; Behroozi et al. 2013), introducing a gas fraction of galaxies into the DMHs (Hopkins et al. 2010; Zavala et al. 2012) and using the luminosity function (Croton 2009). Here we used a combination of semi-empirical and semi-analytic models to seed a black hole in a subhalo/satellite employing the relation  $\sigma$ - $M_{BH}$ .

The number densities of AGNs in groups and clusters can help to establish on firmer ground whether there is any relation between environment density and AGN luminosity (Karouzos et al. 2014), or even the possible two-phase evolution of X-ray AGNs (Miyaji et al. 2015). Figure 2 shows that the satellite subhalos selected have a similar distribution in the two merger scenarios tested, i.e., the shape of the HOD can be described to a good extent by both types of mergers. These processes also approximately reproduce the observed number densities of mXAGNs. The results shown in Figure 2 indicate that minor mergers definitely play a role in establishing the HOD of these AGNs, and point to the necessity of further research on the igniting of AGNs.

While we chose to use  $\lambda_{Edd}=0.1$  based on the median value of the  $\lambda_{Edd}$  distribution from Lusso et al. (2012), it is instructive to show how the results change with  $\lambda_{Edd}$ . Thus, we also estimated simulated HODs for  $\lambda_{Edd} = 0.01, 0.03$  &  $0.3$ . The results are shown in Figure 3, while  $\alpha_s$  values are shown in Table 2. Figure 3 and Table 2 show that the slopes are consistently flat for the minor merger case ( $\alpha_s \approx 0.1 - 0.2$ ) for all  $\lambda_{Edd}$  values, and are consistent with the slopes estimated by Allevato et al. (2012). For the major mergers, the slope becomes steeper ( $\alpha_s \approx 1$  for  $\lambda_{Edd} = 0.01$ ), while it is flat for larger  $\lambda_{Edd}$  values. The global normalization of the minor merger HOD seems to agree better with the observations for  $\lambda_{Edd} = 0.01$  than with higher  $\lambda_{Edd}$  values. However, it is worth noting that the normalization is directly proportional to the AGN lifetime  $\tau_{AGN}$  estimated from Eq. 5, which is a rough approximation. Thus, the agreement or disagreement of the HOD normalization between the models and a few observations should not be used to choose one model over other.

### 5. CONCLUSIONS

In this work, we used cosmological simulations and semi-analytical methods to assign activity to satellite subhalos within halos with mass  $M_{th} \geq 10^{12.75} h^{-1} M_{\odot}$ , and used the merger-driven scenario of BH triggering to obtain an estimate of the contribution of major and minor mergers to the inferred shape of the HOD of mXAGNs.

TABLE 2  
 $\lambda_{\text{EDD}}$  AND  $\alpha_s$

Lambda	Major	Minor
0.01	1.19 $\pm$ 0.16	0.18 $\pm$ 0.04
0.03	0.81 $\pm$ 0.19	0.11 $\pm$ 0.06
0.30	0.54 $\pm$ 0.20	0.15 $\pm$ 0.10

Testing different models can help to constrain the connection between the AGN and the host galaxy as well as the mechanism that triggers its BH. We used an estimate of the duty cycle to associate the number density obtained from the simulated mXAGNs with the observed ones. Our results support the hypothesis that minor mergers, typically not considered as triggering events, can be an important factor in activating mXAGNs.

Our work shows that the HODs of mXAGNs activated by major and minor mergers are very similar and are both consistent, in our approximate treatment, with the flat slope ( $\alpha_s < 1$ ) shape of HOD inferred from observations. The minor merger model reproduces the slope of the satellite HOD of mXAGNs even at  $\lambda_{\text{Edd}}=0.01$ , while that of the major merger model has a steeper slope at this low  $\lambda_{\text{Edd}}$ .

Moreover, since our simulations do not take into account any baryonic processes, other mechanisms such as the ram-pressure stripping of cold gas, are not excluded as a significant cause of the flat slope of the HOD. Our results, however, show that non-baryonic processes such as the decrease of the merging cross-section in the high velocity encounters (Makino & Hut 1997), are at least able to produce a flat slope in satellite HODs.

With the help of large X-ray surveys like eROSITA and larger samples of mXAGNs in groups and clusters, we will be able to constrain the properties of the host of these mXAGNs (e.g., mass); more sophisticated models could lead us to a better understanding of the co-evolution of AGNs and their distribution.

This research was funded by UNAM-PAPIIT project IN108914, IN104113 and CONACyT Research Project 179662. We thank Alexander Knebe for his help with the use of the AHF halo finder and thank Viola Allevato for her discussion of the values of the HOD, as well as Vladimir Avila-Reese for his helpful comments.

## REFERENCES

- Alexander, D. M., & Hickox, R. C. 2012, *NewAR*, 56, 93  
Allevato, V., Finoguenov, A., Cappelluti, N., et al. 2011, *ApJ*, 736, 99  
Allevato, V., Finoguenov, A., Hasinger, G., et al. 2012, *ApJ*, 758, 47  
Arnold, T. J., Martini, P., Mulchaey, J. S., Berti, A., & Jeltema, T. E. 2009, *ApJ*, 707, 1691  
Barnes, J. E., & Hernquist, L. E. 1991, *ApJ*, 370, L65  
Barnes, J. E., & Hernquist, L. 1996, *ApJ*, 471, 115  
Beckmann, V. & Shrader, C. R. 2012, *Active Galactic Nuclei*, (Wiley-VCH Verlag GmbH)  
Behroozi, P. S., Wechsler, R. H., & Conroy, C. 2013, *ApJ*, 770, 57  
Bonoli, S., Marulli, F., Springel, V., et al. 2009, *MNRAS*, 396, 423  
Bournaud, F., Dekel, A., Teyssier, R., et al. 2011, *ApJ*, 741, L33  
Cappelluti, N., Allevato, V. & Finoguenov, A. 2012, *AdAst*, 19, 19  
Ciotti, L., & Ostriker, J. P. 2007, *ApJ*, 665, 1038  
Ciotti, L., Ostriker, J. P., & Proga, D. 2010, *ApJ*, 717, 708  
Cisternas, M., Jahnke, K., Inskip, K. J., et al. 2011, *ApJ*, 726, 57  
Cisternas, M., Gadotti, D. A., Knäpen, J. H., et al. 2013, *ApJ*, 776, 50  
Chatterjee, S., Degraf, C., Richardson, J., et al. 2012, *MNRAS*, 419, 2657  
Chatterjee, S., Nguyen, M. L., Myers, A. D., & Zheng, Z. 2013, *ApJ*, 779, 147  
Chen, Y.-M., Wang, J.-M., Yan, C.-S., Hu, C., & Zhang, S. 2009, *ApJ*, 695, L130  
Coil, A. L., Hennawi, J. F., Newman, J. A., Cooper, M. C., & Davis, M. 2007, *ApJ*, 654, 115  
Coil, A. L., Georgakakis, A., Newman, J. A., et al. 2009, *ApJ*, 701, 1484  
Conroy, C., & White, M. 2013, *ApJ*, 762, 70  
Cox, T. J., Jonsson, P., Primack, J. R., & Somerville, R. S. 2006, *MNRAS*, 373, 1013  
Cox, T. J., Dutta, S. N., Hopkins, P. F., & Hernquist, L. 2008, *ASPC*, 399, 284  
Crocce, M., Pueblas, S., & Scoccimarro, R. 2006, *MNRAS*, 373, 369  
Croom, S. M., Boyle, B. J., Shanks, T., et al. 2005, *MNRAS*, 356, 415  
Croton, D. J. 2009, *MNRAS*, 394, 1109  
da Ângela, J., Shanks, T., Croom, S. M., et al. 2008, *MNRAS*, 383, 565  
Degraf, C., Di Matteo, T., & Springel, V. 2011, *MNRAS*, 413, 1383  
De Robertis, M. M., Yee, H. K. C., & Hayhoe, K. 1998, *ApJ*, 496, 93  
Di Matteo, P., Combes, F., Melchior, A.-L., & Semelin, B. 2007, *A&A*, 468, 61  
Di Matteo, T., Colberg, J., Springel, V., Hernquist, L., & Sijacki, D. 2008, *ApJ*, 676, 33  
Draper, A. R., & Ballantyne, D. R. 2012, *ApJ*, 753, L37



- Ebrero, J., Mateos, S., Stewart, G. C., Carrera, F. J., & Watson, M. G. 2009, *A&A*, 500, 749
- Ehlert, S., Allen, S. W., Brandt, W. N., et al. 2015, *MNRAS*, 446, 2709
- Eke, V. R., Frenk, C. S., Baugh, C. M., et al. 2004, *MNRAS*, 355, 769
- Fanidakis, N., Baugh, C. M., Benson, A. J., et al. 2012, *MNRAS*, 419, 2797
- Fanidakis, N., Georgakakis, A., Mountrichas, G., et al. 2013, *MNRAS*, 435, 679
- Farouki, R., & Shapiro, S. L. 1981, *ApJ*, 243, 32
- Gehrels, N. 1986, *ApJ*, 303, 336
- Gebhardt, K., Bender, R., Bower, G., et al. 2000, *ApJ*, 539, L13
- Georgakakis, A., Gerke, B. F., Nandra, K., et al. 2008, *MNRAS*, 391, 183
- Gilmour, R., Best, P., & Almaini, O. 2009, *MNRAS*, 392, 1509
- Gunn, J. E., & Gott, J. R., III 1972, *ApJ*, 176, 1
- Hasinger, G., Miyaji, T., & Schmidt, M. 2005, *A&A*, 441, 417
- Hernquist, L. 1989, *NYASA*, 571, 190
- Hernquist, L., & Mihos, J. C. 1995, *ApJ*, 448, 41
- Hopkins, P. F., & Hernquist, L. 2006, *ApJS*, 166, 1
- Hopkins, P. F., Hernquist, L., Cox, T. J., et al. 2006, *ApJS*, 163, 1
- Hopkins, P. F., Lidz, A., Hernquist, L., et al. 2007, *ApJ*, 662, 110
- Hopkins, P. F., Hernquist, L., Cox, T. J., & Kereš, D. 2008, *ApJS*, 175, 356
- Hopkins, P. F., & Hernquist, L. 2009, *ApJ*, 694, 599
- Hopkins, P. F., Bundy, K., Croton, D., et al. 2010, *ApJ*, 715, 202
- Hopkins, P. F., Kocevski, D. D., & Bundy, K. 2014, *MNRAS*, 445, 823
- Jiang, C. Y., Jing, Y. P., & Han, J. 2014, *ApJ*, 790, 7
- Jogee, S. 2006, in *Physics of Active Galactic Nuclei at all Scales*, ed. D. Allison, R. Johnson, & P. Liva (Springer: Berlin Heidelberg), 143
- Kaviraj, S. 2014, *MNRAS*, 440, 2944
- Karouzos, M., Jarvis, M. J., & Bonfield, D. 2014, *MNRAS*, 439, 861
- Kayo, I., & Oguri, M. 2012, *MNRAS*, 424, 1363
- Kendall, P., Magorrian, J., & Pringle, J. E. 2003, *MNRAS*, 346, 1078
- Knebe, A., Knollmann, S. R., Muldrew, S. I., et al. 2011, *MNRAS*, 415, 2293
- Knollmann, S. R., & Knebe, A. 2009, *ApJS*, 182, 608
- Kocevski, D. D., Faber, S. M., Mozena, M., et al. 2012, *ApJ*, 744, 148
- Kormendy, J., & Ho, L. C. 2013, *ARA&A*, 51, 511
- Krumpe, M., Miyaji, T., & Coil, A. L. 2010, *ApJ*, 713, 558
- Krumpe, M., Miyaji, T., Coil, A. L., & Aceves, H. 2012, *ApJ*, 746, 1
- Krumpe, M., Miyaji, T., & Coil, A. L. 2014, *Multifrequency Behaviour of High Energy Cosmic Sources*, 71
- Krumpe, M., Miyaji, T., Husemann, B., et al. 2015, arXiv:1509.01261
- Larson, D., Dunkley, J., Hinshaw, G., et al. 2011, *ApJS*, 192, 1
- Leauthaud, A., J. Benson, A., Civano, F., et al. 2015, *MNRAS*, 446, 1874
- Lee, G.-H., Woo, J.-H., Lee, M. G., et al. 2012, *ApJ*, 750, 141
- Lewis, A., Challinor, A., & Lasenby, A. 2000, *ApJ*, 538, 473
- Libeskind, N. I., Yepes, G., Knebe, A., et al. 2010, *MNRAS*, 401, 1889
- Lidz, A., Hopkins, P. F., Cox, T. J., Hernquist, L., & Robertson, B. 2006, *ApJ*, 641, 90
- Lusso, E., Comastri, A., Simmons, B. D., et al. 2012, *MNRAS*, 425, 623
- Makino, J., & Hut, P. 1997, *ApJ*, 481, 83
- Marulli, F., Bonoli, S., Branchini, E., et al. 2009, *MNRAS*, 396, 1404
- Merritt, D., & Ferrarese, L. 2001, *ApJ*, 547, 140
- Mihos, J. C., & Hernquist, L. 1996, *ApJ*, 464, 641
- Milosavljević, M., Merritt, D., & Ho, L. C. 2006, *ApJ*, 652, 120
- Miyaji, T., Zamorani, G., Cappelluti, N., et al. 2007, *ApJS*, 172, 396
- Miyaji, T., Krumpe, M., Coil, A. L., & Aceves, H. 2011, *ApJ*, 726, 83
- Miyaji, T., Hasinger, G., Salvato, M., et al. 2015, *ApJ*, 804, 104
- Mountrichas, G., Sawangwit, U., Shanks, T., et al. 2009, *MNRAS*, 394, 2050
- Mountrichas, G., & Georgakakis, A. 2012, *MNRAS*, 420, 514
- Padmanabhan, N., White, M., Norberg, P., & Porciani, C. 2009, *MNRAS*, 397, 1862
- Porciani, C., Magliocchetti, M., & Norberg, P. 2004, *MNRAS*, 355, 1010
- Pujol, A., & Gaztañaga, E. 2014, *MNRAS*, 442, 1930
- Ramón-Fox, F. G., & Aceves, H. 2014, *Structure and Dynamics of Disk Galaxies*, in *ASP Conf. Ser. 480, Structure and Dynamics of Disk Galaxies*, ed. M. S. Seigar & P. Treuhardt (Petit Jean Mountain, AR) 480
- Richardson, J., Zheng, Z., Chatterjee, S., Nagai, D., & Shen, Y. 2012, *ApJ*, 755, 30
- Sanders, D. B., Soifer, B. T., Elias, J. H., et al. 1988, *ApJ*, 325, 74
- Schawinski, K., Treister, E., Urry, C. M., et al. 2011, *ApJ*, 727, L31
- Shankar, F., Crocce, M., Miralda-Escudé, J., Fosalba, P., & Weinberg, D. H. 2010, *ApJ*, 718, 231
- Shen, Y. 2009, *ApJ*, 704, 89
- Shen, Y., Hennawi, J. F., Shankar, F., et al. 2010, *ApJ*, 719, 1693
- Sijacki, D., Springel, V., Di Matteo, T., & Hernquist, L. 2007, *MNRAS*, 380, 877
- Silk, J., & Rees, M. J. 1998, *A&A*, 331, L1
- Silverman, J. D., Miniati, F., Finoguenov, A., et al. 2014,

- ApJ, 780, 67
- Springel, V. 2005, MNRAS, 364, 1105
- Springel, V., White, S. D. M., Jenkins, A., et al. 2005a, Natur, 435, 629
- Springel, V., Di Matteo, T., & Hernquist, L. 2005b, MNRAS, 361, 776
- Starikova, S., Cool, R., Eisenstein, D., et al. 2011, ApJ, 741, 15
- Taniguchi, Y. 1999, ApJ, 524, 65
- Tapia, T., Eliche-Moral, M. C., Querejeta, M., et al. 2014, A&A, 565, 31
- Thacker, R. J., Scannapieco, E., & Couchman, H. M. P. 2006, ApJ, 653, 86
- Thacker, R. J., Scannapieco, E., Couchman, H. M. P., & Richardson, M. 2009, ApJ, 693, 552
- Treister, E., Schawinski, K., Urry, C. M., & Simmons, B. D. 2012, ApJ, 758, L39
- Tremaine, S., Gebhardt, K., Bender, R., et al. 2002, ApJ, 574, 740
- Ueda, Y., Akiyama, M., Ohta, K., & Miyaji, T. 2003, ApJ, 598, 886
- Ueda, Y., Akiyama, M., Hasinger, G., Miyaji, T., & Watson, M. G. 2014, ApJ, 786, 104
- Van Wassenhove, S., Volonteri, M., Mayer, L., et al. 2012, ApJ, 748, LL7
- Villarroel, B., & Korn, A. J. 2014, NatPh, 10, 417
- Wake, D. A., Croom, S. M., Sadler, E. M., & Johnston, H. M. 2008, MNRAS, 391, 167
- Wyithe, J. S. B., & Loeb, A. 2003, ApJ, 595, 614
- Wyse, R. F. G. 2004, ApJ, 612, L17
- Zavala, J., Avila-Reese, V., Firmani, C., & Boylan-Kolchin, M. 2012, MNRAS, 427, 1503
- Zehavi, I., Zheng, Z., Weinberg, D. H., et al. 2011, ApJ, 736, 59